ADVANCES IN THE HYDROCARBON GAS-LIQUID EQUILIBRIUM UNDERSTANDING IN WATER AND OIL-BASED DRILLING FLUIDS

D. Doninelli, J. Rizzola, P. Gronchi,
Politecnico di Milano, Chemistry, Material and Chemical Engineering Dept. "G. Natta",
L. Da Rù, *Geolog SRL.*

This paper was presented at the 12th Offshore Mediterranean Conference and Exhibition in Ravenna, Italy, March 25-27, 2015. It was selected for presentation by OMC 2015 Programme Committee following review of information contained in the abstract submitted by the author(s). The Paper as presented at OMC 2015 has not been reviewed by the Programme Committee.

ABSTRACT

Aim of this work was to evaluate the concentration of hydrocarbon gases in drilling muds by a static headspace analysis and the hydrocarbon gas-liquid partition coefficient (PC). Aqueous-based muds (salt-saturated and polymer-based) and oil-based (Low-Toxicity OBM) were examined and relation of the gas adsorption and the fluid composition is tentatively proposed. The work wishes to contribute to the knowledge of the desorption kinetics from drilling muds times that is necessary for the mud treatment process. The method is centred on the calculation of the gases' PC starting from the analysis of gas phase at the equilibrium with a known amount of hydrocarbon dissolved in the drilling fluid. A laboratory apparatus was assembled and the analysis was performed at two temperatures: 303 K and at 323 K. The first part (at 303K) included the study of the absorption and desorption of C1-C4 gases. The second part of the experiment focused on pentane. The PC decreases with increasing molecular weight with all mud types, and the phenomenon is controlled more by physical than chemical mechanisms. Further discussion about relation between mud composition and the gas concentrations are also reported. With regards to the effect of temperature, we observed two different behaviours: with the aqueous mud the constant increases with temperature, with oil-base mud it remains constant.

INTRODUCTION

The drilling mud comes into contact with the gas (mainly methane, ethane, propane and C4) in very hard conditions of pressure (hundreds of atmospheres) and temperature (greater than 150°C). Mass transfer phenomena as foams, emulsions or absorptions characterize the gas-liquid interaction. The first two ones depend on mechanical parameters that power the fluid motions, while absorption is both a chemical and chemical-physical phenomena and concerns the direct interaction between gas and liquid molecules. Due to these actions, micro-bubbles of gas are present with dissolved gases (molecular level interaction). As the muds retuns to surface, pressure decreases to ambient values, while the temperature drops to a value which is intermediate between the amabient value and the bottom-hole temperature. At the surface the gases entrained in the drilling fluid are liberated in the atmosphere.

The emission continues with a low rate desorption during the external treatment. After the shale shaker and separation, partial discharge and new filling up operations, the mud is recycled into the well with the original physical density at first properties restored. Considering the mud processing, the analyses of the dissolved and trapped gases is necessary to characterise the mud, to acquire information on the well during the drilling, help to a proper drilling operation and mud itself choice. Thermodynamic models fail to predict the composition at the gas-phase equilibrium due to the great complexity of the system (three phase system with both turbulent and laminar regime) and the phenomenological analysis is the exclusive methodological approach.

The gas detection technique was improved over the years and started to be used to indicate hydrocarbon bearing zones [1]. The extraction of gas from mud is usually performed on gas using gas traps like the QGM (Texaco, 1999), or Constant-Volume gas extractors, in certain cases also

equipped with temperature stabilizers. The analytical procedure generally follows the dynamic head space GC concept. A typical constant-volume extractor utilized by GEOLOG International is shown in fig. 1.
The dynamic analysis is a valid characterisation of muds before the recycle. However the data relative to the mud properties suffer of a high sensitivity to operation parameters (mud sampling, stirring, vessel design, air flux and gas air transportation, time). In fact The some field services use a method that comprehend an heating of the mud sample and provide an air-to-mud ratio, both analytical aspects that are very sensitive on the measure. It does not represent the gas-liquid equilibrium as any quantitative information is available on the dissolved gas at the end of the treatment before the new charge in the well. This work aims to explore an analytical method based on partition coefficient (PC = K_{gl} = C_g/C_l) obtained by the static headspace GC technique [2,3]. The objective is to ascertain the reliability of this procedure useful to establish sets of PC data. The gas-liquid equilibria was deeply examined together to the GC method [4,5] with the aim to calculate in a field, with a single analysis, the low molecular weight (C1-C5) hydrocarbon amounts in the liquid (mud) phase.

Fig. 1. Apparatus for the dynamic head space analysis of gases trapped in the muds (from GEOLOG technical sheet).

EXPERIMENTAL SETUP

MATERIALS

Gas. C1, C2, C3, C4 (99.9950% Vol.) gas calibration standard, were used as purchased from SIAD S.p.A. Linear C5, from Sigma Aldrich as liquid.

Muds. Three kinds of muds, formulated by AVA S.p.A., .were evaluated. Two of these were aqueous, the third oil based. Their composition is described in Tab. 1, 2, 3 of Appendix A.

GAS/LIQUID PARTITION COEFFICIENT.

The gas-liquid partition coefficient (K_{gl}= c_g/c_l where c is mass/volume ratio) relates to the liquid phase solubility of a gas. It is of a practical approach for a temperature dependence evaluation and is measured as weight/volume of the analyte in the gas or the liquid phase ratio.
Considering the relation:

$$m_0 = c_l v_l + c_g v_g$$

where m_0 = *total two phase weight of the analyte; c = gas concentration (weight/volume) in the volume (v) of each phase.*
The PC can be expressed:

$$K_{gl} = \frac{C_g V_l}{m_0 - C_g V_g}$$

The above relation is numerically calculated with the evaluation of the c_g only.

APPARATUS FOR GAS ABSORPTION/DESORPTION.

The gas absorption/desorption apparatus is described in fig. 13 in Appendix B.

TESTS PROCEDURE.

The method was optimized after many tests. 500 ml of mud are fed into the reactor (1/2 reactor volume) and heated at 30°C with the fluid circulated from a thermostatic control unit. The gas is then allowed inside providing that the air volume is completely washed out by purging a gas aliquot. A pressure of 1000 mm H_2O is stabilised. The moles allowed at ($t=t_1$) are calculated by the gas relation:

$$n_i = \frac{\Delta P * V}{\Delta R * T} = \frac{\rho_{H2O} * g * h_0 * V}{R * T} [mole]$$

n_i= 1.95 mmoles if: $\Delta P = 10\ [kPa]$; $V = 500\ [ml]$ reactor head space; $R = 8.314\ [J/mol * K]$ $\rho_{H_2O} = 1000\ [Kg/m^3]$; $g = 9.81\ [m/s^2]$; $h_0 = 1\ [m]$ initial height water column; $T = 30 + 273.15\ [K]$.
The pressure successively decreases due to the liquid absorption, towards an equilibrium value ($t=t_1$). A new gas pressure is adjusted to verify the equilibrium and the observed decreasing registered. The absorbed moles n_{AS} are calculated considering that:
$h_{TOT} = \sum_{i=1}^{K}(h_0 - h_i)$
Where h_i is the height after each refuelling and using the relation

$$n_{AS} = \frac{\rho_{H_2O} * g * h_{TOT} * V}{R * T}\ [mol]$$

The gas mud concentration is then calculated:

$$C_{j,i}^{M,\ IN} = \frac{n_{AS}}{V_{FANGO}}\ \left[\frac{mol}{m^3}\right]$$

The mud is fed into the calibrated vessel to completely replenish it and 5 ml are discharged to create a precise headspace. The glass vessel is maintained at 30°C in a water/alcohol bath. The concentration of the gas is calculated injecting a 0.2 ml gas head space samples in a GC instrument (see after). The small amounts, removed at fixed time), it is assumed does not change the desorption rate or the concentration due to the high liquid/head space volume ratio (5/295).
At similar values of C_i^G, the gas /liquid equilibrium is supposed and, from a mass balance, the gas concentration ***i*** in the ***j*** mud,

$$C_{j,i}^{M,\ IN}$$

It is then possible to know both the moles in the mud and those in the gas phase.
$n_{J,i}^{M,\ IN} = C_{J,i}^{M,\ IN} * 0.295 * 10^{-3}\ [mol]$
$n_i^G = C_i^G * 0.005 * 10^{-3}\ [mol]$
The moles in the mud at the equilibrium are:
$n_{J,i}^{M,\ EQ} = n_{J,i}^{M,\ IN} - n_i^G\ [mol]$
From which
$C_{J,i}^{M,\ EQ} = \frac{n_{J,i}^{M,\ EQ}}{V_{beuta}=0.295*10^{-3}}\ \left[\frac{mol}{m^3}\right]$

The PC is

$$K_{J,i}^{EQ,G/L} = \frac{C_i^G}{C_{J,i}^{M,\ EQ}}$$

GC ANALYSIS

A HP 5890 serie 2 GC instrument equipped with a 30 m capillary glass column Restek-Rt-Q-Bond, 0.32 mm i.d., with a 10 µm absorption layer (100% divinilbenzene). The analyses were performed with an increasing temperature method with 1 min at 30°C and then a 35°C/min ramp to 280°C (1 min).

An example of the analysis is reported in fig. 2. Calibration was repeated every 25 analysis and the molecular weight deposit washings executed at high temperature.

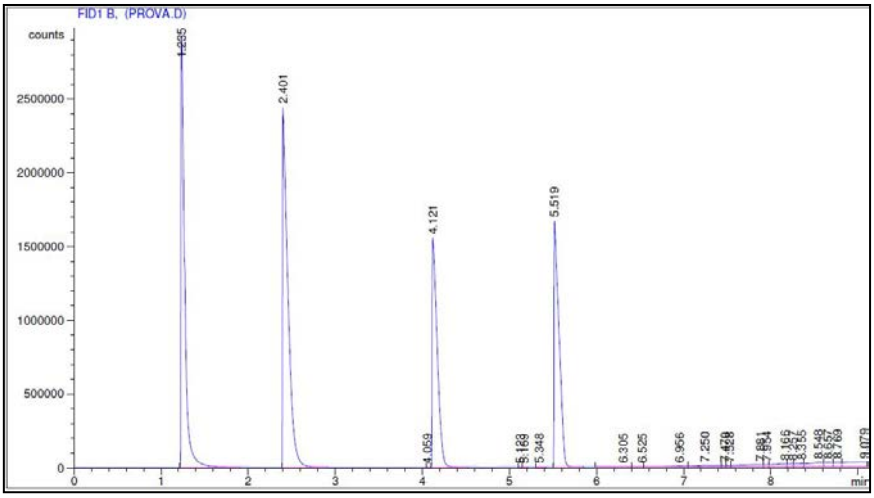

Fig. 2. Example of a GC C1-C4 hydrocarbons analysis.

RESULTS

The graph of fig. 3 is reported as one example of the desorption of hydrocarbon from the mud. It relates to the rate of the absorption of methane interacting with the PHPA mud. The absorption in the aqueous mud is very slow at the imposed conditions and it begins after 6-7 hours under stirring.

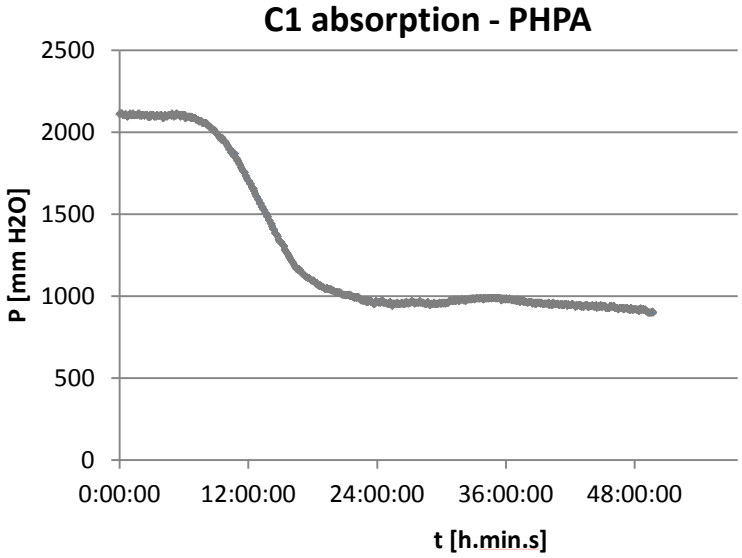

Fig. 3. *C1* absorption rate.

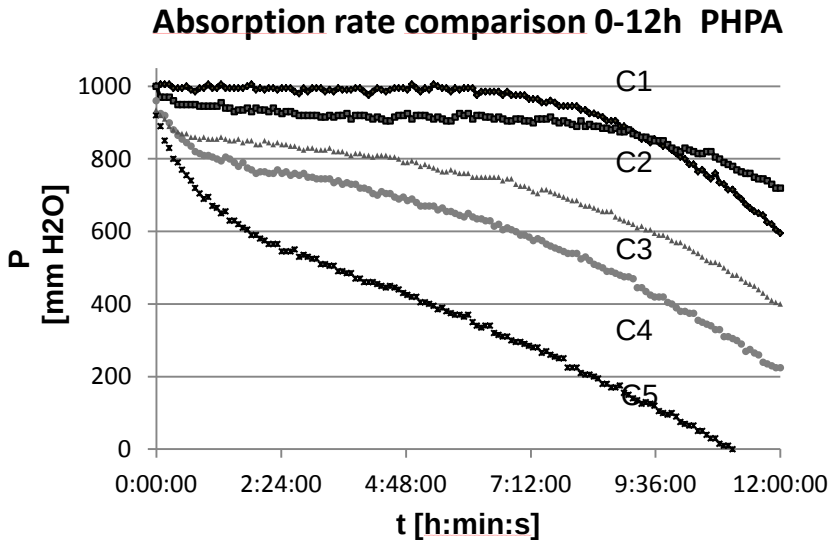

Fig. 4. 12h comparison among the C1-C5 hydrocarbons at 50°C (B) from continuous data logging.

The graph of fig. 4 compares the rate of initial absorption for each gas at 50°C. The rate clearly depends on the vapour pressure of the gas being greater for C5 hydrocarbon that shows the maximum absorption rate after few minutes from the pressure. The absorption rate decreases with the hydrocarbon chain length and methane is adsorbed only after 12 hours.
According our analysis, more relevant to note, is the desorption rate. The graphs reported in fig. 5 relate to the desorption rates in the first hour. Generally it appears that the rate depends on the mud and on the hydrocarbon: the C4 hydrocarbon desorbs more quickly from the LT-OBM oil muds than the C2 (or C3) one from the HPWBM (or PHPA) mud that contain more organic component notwithstanding the greater vapour pressure of the ethane and propane.

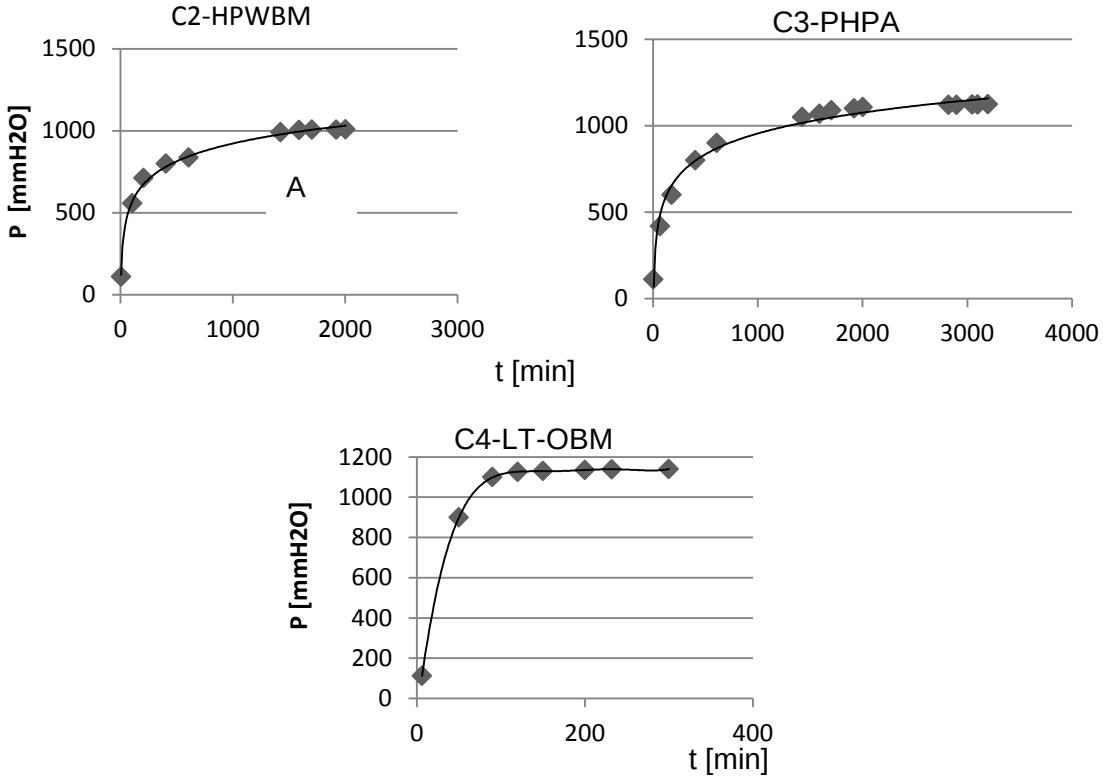

Fig. 5. Gas desorption at 30°C from different muds.

A different desorption rate dependence on the vapour pressure is observed. Due to the procedure (see the experimental part), the results obtained by the GC analysis after the reaching of the gas-liquid equilibrium, refer to the gas dissolved into the muds and not to the gas trapped into the micro-bubbles.

MUD DEPENDENCE OF THE PARTITION COEFFICIENTS (PC).

Table 1 and 2 reports the values of the PC (as K_{gl}) calculated at 30° and 50 °C respectively. The values in the square brackets represents the mean uncertainty percent A significant difference exists between the two temperature as at 30°C the values are one half or one third of those at 50°C. The brackets near the values indicate the square mean deviation as percent. These are greater for low carbon methane and ethylene when calculated for the PHPA mud meaning an analytical sensitivity for high volatile compounds.

Tab. 1. Partition coefficients (PC; K_{gl}) at 30°C.*

	Mud		
Hydrocarbon	***PHPA***	***HPWBM***	***LT-OBM***
C1	5.86 [18]	0.48 [5]	0.87 [3]
C2	2.81 [15]	0.30 [4]	0.29 [2]
C3	1.93 [5]	0.12 [4]	0.20 [2]
C4	1.64 [5]	0.09 [2]	0.09 [1.5]

Tab. 2. Partition coefficients (PC; K_{gl}) at 50°C.

	Mud		
Hydrocarbon	***PHPA***	***HPWBM***	***LT-OBM***
C1	*13,00* [16]	9,81 [7]	7,31 [5]
C2	12,54 [9]	8,16 [5]	6,28 [4]
C3	8,60 [5]	4,24 [4]	1,45 [5]
C4	4,67 [5]	0,85 [5]	0,55 [5]
C5	4,39 [5]	1,22 [5]	0,31 [4

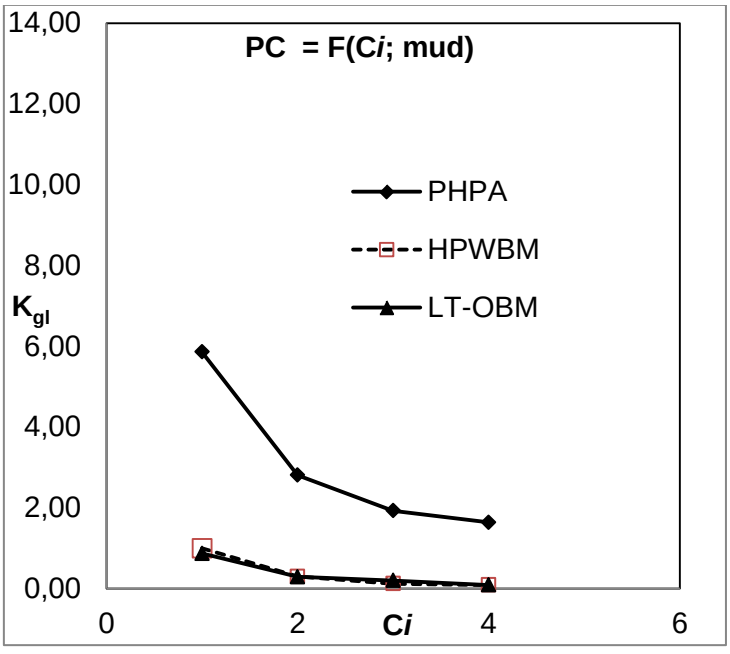

Fig. 6. Partition coefficients (K_{gl}) at 303 K.

Fig. 6 and 7 represents the same data allowing a better, quick, appreciation of the dependence of PC on the mud kind and molecular weight of hydrocarbon. The C5 hydrocarbon behaviour was not evaluated at 30°C.

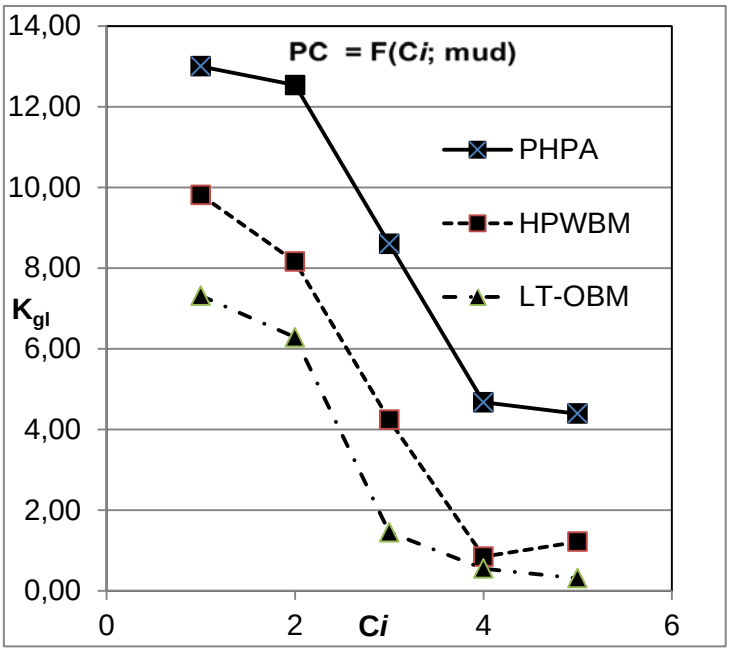

Fig. 7. Partition coefficients (K_{gl}) at 323 K.

Observing the ideal curve of values belonging to the same mud clearly appears that an increasing of the molecular weight causes a net decrease of the PC from C1 to C3. Then it seems to stabilize. The influence of the mud composition is more pronounced at 50°C; generally the data differentiate greatly each to other. The behaviours of HPWBM and LT-OBM muds appears almost the same at 30°C.

TEMPERATURE DEPENDENCE OF PARTITION COEFFICIENT

The solubility of gases in liquids changes with temperature variation.

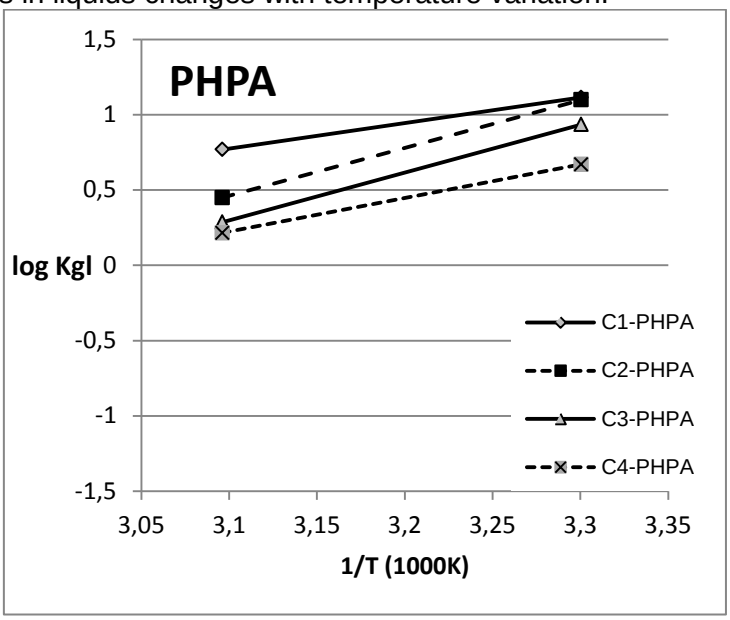

Fig. 8. Van't Hoff Equation; PHPA mud; two partition coefficients, PC, at 30 and 50°C

Therefore partition coefficient is dependent on temperature. Theoretically, the partition coefficient obeys a thermodynamic model as given by the van't Hoff Equation:

$$log\ K_{gl} = -\Delta F/2.303RT+C$$

where ΔF, R, T, and C are the free energy of transfer from liquid to the gas phase, the gas constant, the temperature, and a constant, respectively.
According to the model, a plot of log K_{gl} versus 1/T gives a straight line. From the slope of the linear regression, the difference of the energy activation of the transfer can be calculated between two temperatures using the Arrhenius model.
The van't Hoff model is used to design the graphs reported in fig. 8, 9, and 10. They are based on two single temperature points only. At first, it is evident a greater similitude among the *log Kgl-1/T* relations for each hydrocarbon in the PHPA mud than the other two ones, where the lines are more separated each other, probably indicating a similar interaction of all the hydrocarbon with the water based mud. Moreover the positive log K_{gl} (negative free energy) values confirm that the activity in the gas phase is favoured in the PHPA mud (fig. 8). From the comparison of the free transfer energy with PHPA, with the other two muds it appears that the hydrocarbon dissolved more likely in HPWBM and LT-OBM muds. (Appendix C) where, on the contrary the log K_{gl} is negative at 303 k (fig. 9 and 10).

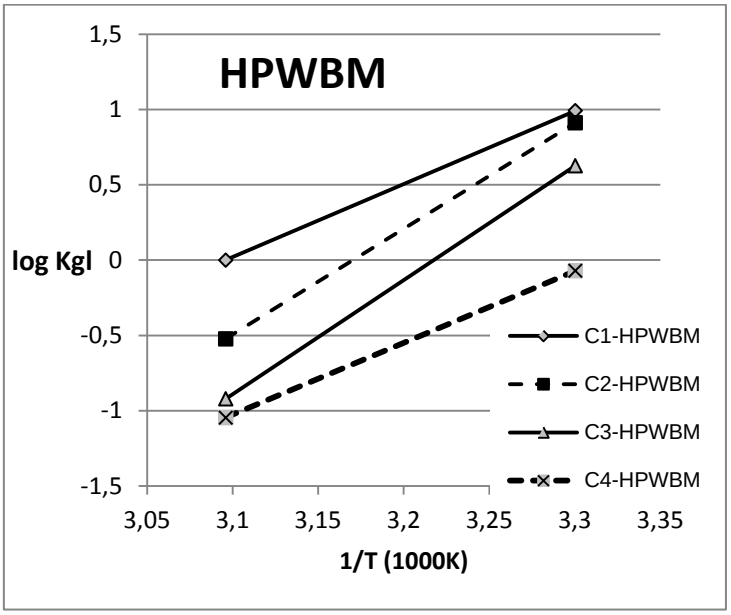

Fig. 9. Van't Hoff Equation; HPWBM mud; two partition coefficients, PC, at 30 and 50°C

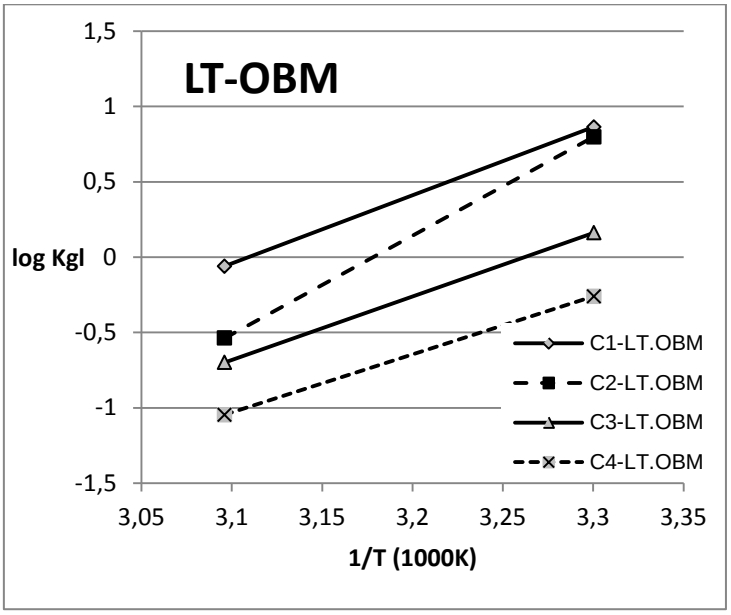

Fig. 10. Van't Hoff Equation; LT-OBM mud; two partition coefficients, PC, at 30 and 50°C

Morever all the free energy data decrease by increasing the hydrocarbon chain according to a greater solubilty of longer chain. The observation agrees with a low solvation of hydrocarbons in water than organic based muds (lower affinity due to the lower polarity).
As an example, fig. 11 relates to the C1 only hydrocarbon and indicates the K_{gl}-T relation for the different muds. Again the PHPA mud shows a different behaviour respect to the other two ones.

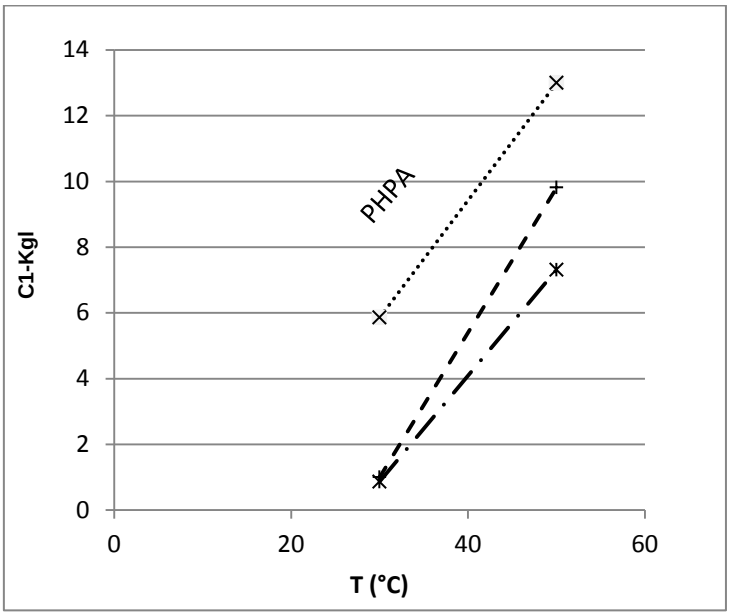

Fig. 11. Van't Hoff model for the C1 Hydrocarbon for different muds.

DISCUSSION

The aim of this work was to explore the reliability of a static headspace GC analysis of the gas content in a drilling mud at equilibrium conditions before the recycle into the well. Others authors have conceptualised what is happening from the zone of the drilling from the bottom-hole and the well-head limiting the exam to water born fluids [6]. The reason was that in petroleum reservoirs the aqueous liquid phase always coexists with hydrocarbons in high pressure/high temperature conditions and their solubility in water is such that it cannot be neglected [7]. Regarding the mud treatment after the drilling, the evaluation of the degassing of the mud between the well-head and the gas-trap has been also promised based on experiment data obtained by two gas-traps situated along the mud processing line out the well, but from the year 2006 nothing appear in the literature.
The gas system however is very complex to analyse as existing data on pure hydrocarbon cannot be used due to the multicomponent nature and the subsequent interactions [8, 9, 10]. This work therefore examined experimental data only relating to the absorption and desorption aspects too.
In fact the gas-liquid properties change when non-aqueous muds are used and, moreover, greater gas solubility is expected and that may overcomes the thermodynamic value as proved by the rapid initial desorption (a kinetic aspect) of C4 from the oil based mud. The different surface tension of the muds at increasing of the organic component greatly changes and the foam phase volume increases. In fact our data indicate that the total amount of desorbed gas decreases with the organic component of the mud i.e. the dissolved amount increases (Fig. 10 and Tab. 3).

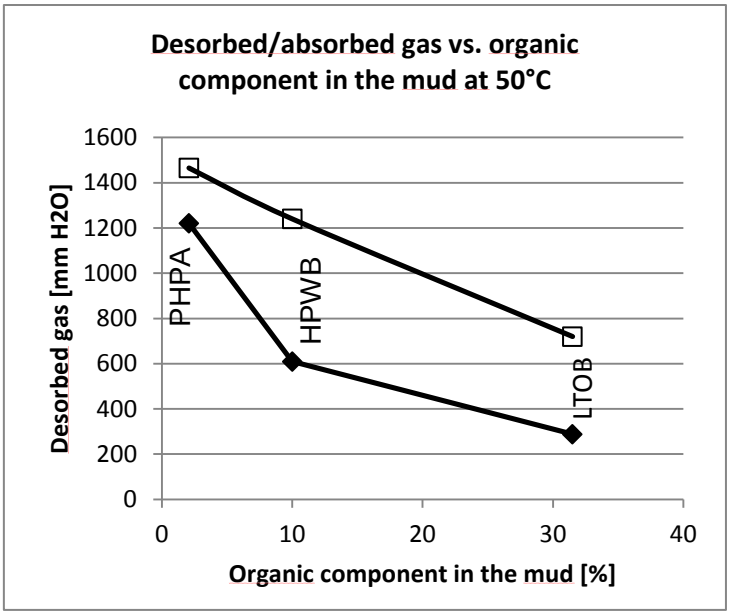

Fig. 12. Graphical comparison between the absorbed (hollow marks) and desorbed (filled marks) amounts.

Tab. 3. Absorbed and desorbed amounts.

MUD	%	Abs. (mmH_2O)	Des. ($mm\ H_2O$)	Abs/Des	Δ (Abs-Des)
PHPA	2.1	1465	1222	1.20	243
HPWBM	10.0	1180	609	1.94	571
LTOBM	31.5	730	288	2.53	442

As a consequence one supposes a relevant gas degassing due to the gas in the micro-bubbles. The gas rapidly leaves the muds in the flash immediately after the well, but, as we observed analysing the desorption rate and at the equilibrium completely reached only after 2 hours. It is likely to suppose that the remaining gas is the gas only dissolved by the chemical interactions with the mud component.

Together to a greater understanding of the gas-liquid equilibria, this study is aimed to suggest one analytical procedure to help the rapid determinations (semi-continuous mode) of the gas amount not desorbed from the mud. The knowledge of the partition coefficient is believed to be a straight way to be applied in field. This choice initially requires a very large experimental effort to build graph and chart reporting the partition coefficient and their variation with the temperature. Nevertheless the calculation of the gas in the liquid phase is after very quick.

Our experimental procedure starts creating a *Ci* hydrocarbon saturated mud. The second part of the test was the creation of a head space, the analysis of the desorption time until the phase equilibrium and the quantitative determination of the gases at this point. After a simple calculation the gas dissolved in the liquid is easy known.

The method suffers of a high sensitivity as, considering the literature [3, page 282], at low K_{gl} values the dependence to the liquid volume sampled is highly variable. We choice a liquid/head space ratio of 295 to decrease the sensitivity [2].

The partition coefficient data, reported in fig. 6 and 7, agree with an increasing of the solubility at great molecular weight at a first sight proportional with the vapour pressure of the gas. The dependence from the temperature, reported in fig. 8, 9, 10 following the Arrhenius law, also agree with thermodynamic basic concerns.

CONCLUSIONS

The interaction of gases with mud during drilling is such that the gas reaches the surface both as gas trapped in micro-bubbles and dissolved into the liquid phase. Further interaction with cuttings complicates the physical interpretation. The static headspace analysis may be utilised to tracks precise quantitative analysis on the dissolved part of gas.

The method adds information on all the characterisation normally acquired by the mud logging service (penetration rate, lithology, and total gas mud content, individual hydrocarbon compounds) allowing calculating the flashed gas.
The work allows a deeper understanding of what is the absorption and desorption behaviour whose knowledge cannot be eluded when studying the gas-liquid equilibrium.
The method procedure for a rapid analysis on field passes through the determination of partition coefficients and their dependence on temperature. The work here presented needs a more hard analytical work, but at this stage, it appears a promising start point for a useful comprehension of gas-mud interaction in order to a greater proper choice of formulation and for the evaluation of gas trapped in a dissolved mode in the mud. The authors believe that the gas analysis in this complex systems must be studied starting from the experimental analysis first.

ACKNOWLEDGEMENTS

The authors wish to acknowledge GEOLOG Surface Service for the financial support given trough the research contract with the Politecnico di Milano.

REFERENCES

[1] Bell, P. A. C., and al., “The expanding role of mud logging”, *Oilfield Reviews*, Schlumberger, 2012, 24(1), pp. 24-41.

[2] Lomond, J. S., Tong, A. Z., “Rapid Analysis of Dissolved Methane, Ethylene, Acetylene and Ethane using Partition Coefficients and Headspace-Gas Chromatography”, *Journal of Chromatographic Science,* Wolfvile, Canada:, July 2011, vol. 49.

[3] Penton, Z.E. “ Head space gas Chromatography” in *“ Sampling and Sample Preparation for Field and Laboratory*”, Elsevier, Boston-Amsterdam, 2002, vol. 37, Chapter 10.

[4] Cicero, V. Torsello, M. A., Valutazione sperimentale della solubilità di idrocarburi leggeri (C1-C4) in fanghi di perforazione, *Thesis*, Politecnico di Milano, AA 2012-13.

[5] Doninelli, D., Rizzola, J., Studio dell'equilibrio gas-liquido di idrocarburi C1-C5 nei fanghi di perforazione, *Thesis*, Politecnico di Milano, AA 2013-14.

[6] Liège, X. C., “Dissolution of light hydrocarbons in drilling muds, prediction of the nature of a reservoir fluid based on Gas Shows”, *PhD. Dissertation,* University of Denmark, DK-2800 Lyngby, May 2006*,* Denmark, pp. 1-265.

[7] Dhima, A., de Hemptinne, J.C., Moracchini G.,”Solubility of light hydrocarbons and their mixtures in pure water under high pressure”, *Fluid Phase Equilibria*, Elsevier, 1998, March, vol. 145(1), pp.129–150.

[8] Amirijafari, B., “Solubility of light hydrocarbons in water under high pressures”, *PhD thesis*, The U. of Oklahoma, Norman, 1969.

[9] Amirijafari, B., Campbell, J., “Solubility of gaseous hydrocarbon mixtures in water”, *Soc. Pet. Eng. J.*, SPE, 1972, pp. 21–27.

[10] Leinonen, P.J., Mackay, D., “The multicomponent solubility of hydrocarbons in water**”,** *Can. J. Chem. Eng.*, 1973, vol. 51, pp. 230–233

APPENDIX A

Legend: V = viscosifier; SH = Shale-control Agent; LU = Lubricants; FR = filtration reducer; HPHT = High pressure/High temperature; HPWB = High Performance Water-based; W = Weighting Materials; E = emulsifiers; TE = temperature stability agent; SU = Surface-active agents;

Tab. 4. PHPA formulation

Additive	kg/ m^3	% w/w	Function		
Fresh water	*884*	70.72			
NaOH	*1*	0.08			
Na_2CO_3	*2*	0.16			
KCl	*40*	3.2			
Visco XC84	*3*	0.24	*V*	*SH*	
Visco 83 XLV	*6*	0.48	*FR*	*SH*	
Ecolube	*10*	0.8	*LU*	*SH*	
Polivis	*7*	0.56	*V*	*SH*	*HPHT*
Barite	*297*	23.76			

Tab. 5 HPWBM formulation.

Additive	kg/ m^3	% w/w	Function		
Fresh water	*805*	64.4			
NaOH	*3*	0.24			
Na_2CO_3	*3*	0.24			
KCl	*30*	2.4			
Visco XC84	*4*	0.32	*V*	*SH*	
Visco 83 XLV	*6*	0.48	*FR*	*SH*	
Avagreenlube	*15*	1.2	*LU*	*SH*	*FR*
Avapolyoil	*80*	6.4	*SH*	*LU*	*HPWBM*
Avaperm NF	*10*	0.8	*SH*		
Avalig NE	*10*	0.8	*W*	*SH*	*HPHT*
Barite	*284*	22.72			

Tab. 6. LT-OBM formulation

Additive	kg /m^3	% w/w	Function		
Lamix	*382*	*22.54*			
Avoil PE/LT	*18*	*1.06*	*E*	*FR*	*SU*
Avoil SE/LT	*18*	*1.06*	*E*	*FR*	*TE*
Avoil WA	*4*	*0.24*	*SU*	*E*	
Avoil FC	*13*	*0.77*	*FR*	*E*	*SU*
Brine CaCl2@1.19 sg	*206*	*12.16*			
Lime	*30*	*1.77*			
Avabentoil SA	*15*	*0.89*	*V*	*FR*	
Avabentoil HY	*4.5*	*0.27*	*V*	*FR*	*HPHT*
Rev Dust	*100*	*5.90*			
Barite	*904*	*53.35*			

APPENDIX B

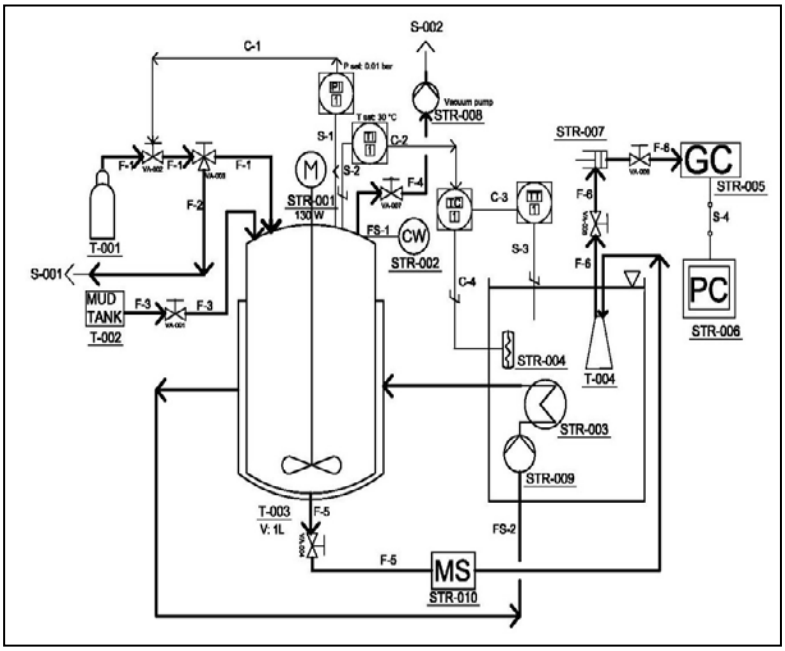

Logic connexion	Role
PI-1	Pressure Indicator
TI-1	Temperature indicator.
TC-1	Temperature indicator and control.
TT-1	Temperature trasmission.
S-1	Pressure trasmission
C-1	Pressure manual control
S-2	Electric cable
C-2	Temperature manual control
S-3	Electric cable
C-3	Electric cable
C-4	Electric cable
S-4	PC-GC connession

Fluxes on P&I	Role
F-1	Gas IN.
F-2	Air flux OUT
F-3	Mud fluid IN
F-4	Air flux OUT
F-5	Mud flux to sampling
F-6	Gas to analysis
FS-1	Cool water flux
FS-2	Warm water

Item	Role
STR-006	Personal computer for GC calculation
STR-007	Gas sampling device.
STR-008	Vacuum system for mud transfer.
STR-009	Jacket circulation pump of water.
STR-010	Mud Manual sampling.
S-001	Air vent.
S-002	Air vent..
VA-001-2-4-5-6-7	Valve.
VA-003	Three way valve.

Item	Role
T-001	Gas reservoir
T-00	Fluid tank
T-003	Jacketed absorption reactor
T-004	Gas-saturated mud tank
STR-001	Motor for stirring
STR-002	Reactor head cooling system
STR-003	Heat exchanger at reactor jacket.
STR-004	Water heating system
STR-005	Quantitative analysis for gases from sample saturated mud.

Fig. 13. Laboratory apparatus for absorption/desorption.

APPENDIX C

Tab. 7.Transfer free energy (F) from liquid to gas phase

PHPA	ΔF (cal/mole)			
T(K)=303	-1060,98	-619,96	-394,54	-296,84
T(K)=323	-1640,68	-1617,42	-1376,31	-986,18
HPWBM	ΔF (cal/mole)			
T(K)=303	0,00	722,44	1272,26	1444,88
T(K)=323	-1460,75	-1342,61	-923,78	103,96
LT-OBM	ΔF (cal/mole)			
T(K)=303	83,56	742,78	965,74	1444,88
T(K)=323	-1272,81	-1175,44	-238,33	382,41